

THERMAL EFFICIENCY ANALYSIS OF THE ROTARY KILN BASED ON THE WEAR OF THE LINING

Donghu Zeng and V. Yu. Shcherbina*

Department of Chemical, Polymer and Silicate Engineering, Faculty of Chemical Engineering,
National Technical University of Ukraine, Kyiv, 03056, UKRAINE
E-mail: xpsm@ukr.net

Jiaxiu Li

Department of Economic and Social Geography, Faculty of Geography,
Taras Shevchenko National University of Kyiv, Kyiv, 01033, UKRAINE

The thickness of the lining is reduced from 230 mm to 80 mm due to long-term wear, resulting in low thermal efficiency of the rotary kiln. The thermal resistance, which is positively correlated with the thickness of the lining, is one of the most important factors determining the thermal efficiency of the rotary kiln. The thermal efficiency of the rotary kiln can be improved by introducing insulation material with lower thermal conductivity into the lining. The average heat flux is used as the thermal efficiency evaluation index of the 4×60 m rotary kiln under no-load conditions in this work. A numerical experiment was conducted for the temperature and heat flux of the inner surface of the lining, as well as the temperature of the outer surface of the shell during the wear of the lining. There are two cases considered, one with and one without insulation materials in lining. According to the analysis, when the lining in the high temperature zone of the rotary kiln wears to 80 mm, the average heat flux of the inner surface of the lining increases by 105.03%. However, after the addition of insulation material, the average heat flux on the inner surface of the lining increases by 40.33% (wears to 80 mm). Compared to the thermal efficiency of the rotary kiln without heat insulation material, the average heat flux of the inner surface of the lining is reduced by 36.36% (230 mm), and it is reduced by 99.01% (wears to 80 mm). A significant advantage of this solution is that it can increase the thermal efficiency of the rotary kiln, improve the insulation performance of the lining, reduce heat loss to the environment through the shell, and the results obtained can be used for the latest equipment design and existing equipment improvements.

Keywords: rotary kiln, thermal efficiency, average temperature, heat flux, insulation material.

1. Introduction

Modern cement [1] has always been considered an indispensable building material in the field of housing and infrastructure [2, 3], which evolved on the basis of ancient cementitious materials [4]. Rotary kilns, which are widely used [5] in the cement industry where they are well suited for the cement clinker burning processes that require high temperatures at near-atmospheric pressure [2, 6], are industrial thermal equipment working in the temperature range between 200 – 2000° C [7]. Due to excellent mixing performance, efficient heat transfer capability and great installed capacity of the rotary kiln [8], it is employed in many engineering applications such as drying, cement making, melting, cooling, recycling of waste and destroying of hazardous substances [9-12].

During long-term operation of the rotary kiln, the thickness of the lining gradually decreases from 230 mm to 80 mm and due to wear [13] between the bulk raw material and the lining, resulting in the breakdown of the working layer of the lining and the fall of the refractory brick from the lining after wear of about 30 – 40% [14]. At the same time, the thermal resistance of the lining also decreases accordingly, because

* To whom correspondence should be addressed

it is positively correlated with the thickness of the lining. This is why the thermal efficiency of the rotary kiln is low which means a corresponding increase in energy consumption, electricity usage and greenhouse gas emissions [15]. Approximately 20 to 35% of the total heat from the combustion of the fuel is released into the environment through the shell of the rotary kiln [16-18]. In Ukraine, most cement clinkers are processed in rotary kilns, which have a low fuel utilization rate from 55 to 60%. Therefore, improvement of the thermal efficiency in a rotary kiln is extremely crucial for the nation, region and the building sector, meanwhile finished product quality, cost of rotary kiln making, service life and environmental protection all must be taken into consideration.

The purpose of this work is to investigate the impact of the wear of the lining on the thermal efficiency of the rotary kiln based on the absence of filling of the bulk raw materials and to propose a realistic solution to prevent the thermal efficiency reduction. To properly analyze the thermal efficiency of the rotary kiln during the wear of the lining, the thermal resistance, temperature field, and heat flux of the rotary kiln are examined in this work using the first and second laws of thermodynamics. Thermal resistance [19] is well known to be one of the most prominent factors determining the heat transfer capacity or insulation performance in the rotary kiln [22, 24] and the parameters that influence thermal resistance are the distance of heat transfer and thermal conductivity. Thermal resistance of the rotary kiln steadily diminishes with wear of the lining, diminishing the thermal efficiency of the rotary kiln. Since the thickness of the lining is reduced from the original 230 mm to 80 mm because of wear, in this work we study the thermal efficiency of the rotary kiln with the thickness of the lining of 230 mm, 200 mm, 170 mm, 140 mm, 110 mm and 80 mm, respectively. This uniqueness of this work was that it also examines the thermal efficiency of the rotary kiln following the addition of the trapezoidal insulation material which has a better stability than other shapes with the height of the lining corresponding to the above mentioned. The trapezoidal insulation material was built in the center area of the refractory brick of the lining for fabricating a more heat-resistant lining of the rotary kiln [25, 26]. Without making significant changes to the design of the rotary kiln, this solution can reduce the heat loss of the rotary kiln to the environment through its shell and improve its thermal efficiency. The necessary relevant data were collected from a simulation of the VESNA created by the Department of HPSM at the National Technical University of Ukraine, and part of the data came from the Kryvyirig Cement Plant in Ukraine.

2. Material and methods

Thermal resistance of the lining is determined by both the height HI and thermal conductivity of the lining. The thicker the height HI of the lining and the lower thermal conductivity of the lining, the bigger the thermal resistance, and thus the higher the thermal efficiency of the rotary kiln. However, as the lining thins because of long-term wear of both the lining and bulk raw materials, the heat transfer distance shortens, lowering thermal resistance and thermal efficiency. In this work, to increase the heat resistance of the lining of the rotary kiln, and hence increase the efficiency, insulation materials with lower thermal conductivity must be introduced into the rotary kiln.

Given that the rotary kiln can be divided into distinct temperature zones, such as the drying zone, preheating zone, calcining zone, burning zone, and cooling zone, it is worth noting that the temperature in the burning zone can reach higher levels (ranging from 1300 to 1700°C) than in the other zones. Thus, this work was carried out specifically on the burning zone, where the kiln operates under extreme conditions without bulk raw material present, to conduct a comprehensive investigation of the thermal processes that occur within the rotary kiln and to assess the thermal efficiency of the rotary kiln. Two different cases were considered, namely: with and without insulation materials in the lining of the rotary kiln.

Because the temperature field and heat flux of each annular area of the rotary kiln are the same without filling bulk raw materials, therefore, in this study, only one refractory brick from the burning zones in the rotary kiln and the corresponding shell were taken as the research object. The thermal efficiency of the rotary kiln can be numerically described employing $T_{av}^L(i)/T_{av}^{L+In}(i)$, $T_{av}^S(i)/T_{av}^{S+In}(i)$ and $q_{av}^L(i)/q_{av}^{L+In}(i)$ as shown in Fig.1. When $T_{av}^L(i)/T_{av}^{L+In}(i)$ rises, $T_{av}^S(i)/T_{av}^{S+In}(i)$ drops, and $q_{av}^L(i)/q_{av}^{L+In}(i)$ reduces, this means that the thermal efficiency increases. Additionally, the maximum temperature is distributed on the inner surface of the

lining, while the minimum temperature is distributed on the outer surface of the shell due to the principle of heat transfer from a higher temperature medium to a lower temperature medium.

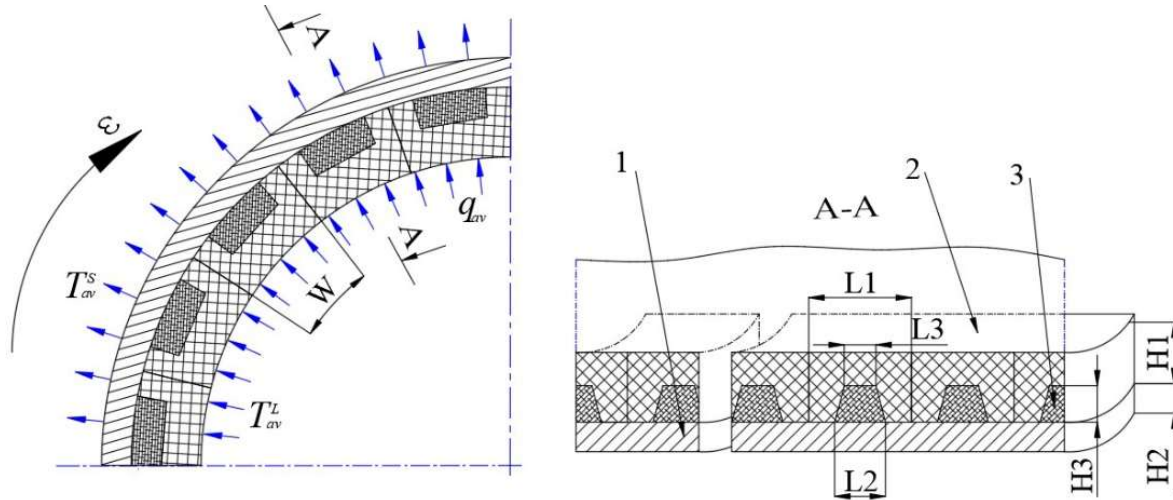


Fig.1. Scheme of heat exchange in the transverse and longitudinal sections of the rotary kiln:
 1 - the shell; 2 - the lining; 3 - the trapezoidal insulation material.

The rotary kiln utilized in the Kryvyirig cement plant in Ukraine has a radius of 2 m . This study set the shell materials as hydrocarbon steel, the lining to be Chamotte, and the insulation material as Chamotte, and the insulation material as Mullite-silica fiber, as shown in Tab.1.

Table 1. Physical property parameters.

	Thermal conductivity(λ) $W/m\cdot K$	Maximum temperature $^{\circ}C$
Hydrocarbon Steel	45.5 (λ_S)	538
Chamotte	1.16 (λ_L)	1600
Mullite-Silica Fiber	0.15 (λ_{In})	1400

During the operation of the rotary kiln, $T_{max}^L(i)/T_{max}^{L+In}(i)$, $T_{max}^S(i)/T_{max}^{S+In}(i)$ and $T_{max}^{In}(i)$ cannot exceed the maximum temperature of its own physical properties, otherwise it will fail and cause major safety accidents.

The heat transfer process of the rotary kiln in this study involves heat convection, heat conduction, and heat radiation [8]. Heat convection occurs at the contact surface between the high-temperature hot gas flow and the lining, as well as the environment and the shell. At the contact surface between the environment and the shell, heat radiation occurs. Here conduction occurs in the lining, shell, and insulation material (if included). The thermal conductivity of the lining, shell, and insulation material is shown in Tab.1. In this study, the Dirichlet boundary condition is used in the rotary kiln because the initial temperature of the rotary kiln is given ($T = T_0$). The initial temperature of the inner surface of the lining (inner boundary) was determined by the temperature of the high-temperature gas flow inside the rotary kiln from experimental dependences, in this work the initial temperature of the inner surface of the lining was taken to be 1700°C as extreme condition, while the initial temperature of the outer surface of the shell (outer boundary) was determined by the temperature of the environment (20°C).

Since the linear expansion coefficient of the lining is 5-6 times higher than that of the shell, the lining is in full contact with the shell [26, 27], the insulation material is also in full contact with the lining.

Accordingly, the boundary conditions of the contact area between the lining and the shell are:

$$T_{L-OuterSur} \Big|_{r=\frac{D_P+H_1}{2}} = T_{S-InnerSur} \Big|_{r=\frac{D_P+H_1}{2}}, \quad (2.1)$$

$$\lambda_L \frac{\partial T_{L-OuterSur}}{\partial r} \Big|_{r=\frac{D_P+H_1}{2}} = \lambda_S \frac{\partial T_{S-InnerSur}}{\partial r} \Big|_{r=\frac{D_P+H_1}{2}}.$$

In the contact area of the lining with the insulation material:

$$T_L \Big|_{r=H_3, L_3} = T_{In} \Big|_{r=H_3, L_3}, \quad \lambda_L \frac{\partial T_L}{\partial r} \Big|_{r=H_3, L_3} = \lambda_{In} \frac{\partial T_{In}}{\partial r} \Big|_{r=H_3, L_3}. \quad (2.2)$$

The efficient heat transfer coefficient $h_{S \rightarrow E}$ between the corresponding shell and the environment was given [10, 20]:

$$h_{S \rightarrow E} = 3.5 + 0.062 T_{S-OuterSur}. \quad (2.3)$$

Expression [21] can be used to calculate the efficient heat transfer coefficient $h_{G \rightarrow L}$ from the high-temperature hot gas flow to the inner surface of the lining:

$$h_{G \rightarrow L} = \frac{5.68 \varepsilon_L}{T_G - T_{L-InnerSur}} \left[\varepsilon'_G \left(\frac{T_G}{100} \right)^4 - \varepsilon''_G \left(\frac{T_{L-InnerSur}}{100} \right)^4 \right] + \frac{0.418 \cdot \lambda_G}{D_P} \left(\frac{\omega_G D_P}{v_G} \right)^{0.67}. \quad (2.4)$$

Formula (2.3) can be used to calculate the thermal resistance R with the length L_1 of the refractory brick from 0 mm to 150 mm without the insulation material.

$$R = \left(\frac{1}{h_{G \rightarrow L}} + \frac{H_1(i)}{\lambda_L} + \frac{H_2}{\lambda_S} + \frac{1}{h_{S \rightarrow E}} \right) \frac{X}{X}, \quad 0 \leq X \leq L_1. \quad (2.5)$$

The thermal resistance R_{In} is calculated after introduction of the trapezoidal insulation material:

- for $0 \leq X \leq \frac{L_1 - L_2}{2}$

$$R_{In} = \left(\frac{1}{h_{G \rightarrow L}} + \frac{H_1(i)}{\lambda_L} + \frac{H_2}{\lambda_S} + \frac{1}{h_{S \rightarrow E}} \right) \frac{X}{X}, \quad (2.6a)$$

- for $\frac{L_1 - L_2}{2} < X \leq \frac{L_1 - L_3}{2}$

$$R_{In} = \frac{1}{h_{G \rightarrow L}} + \frac{H_1(i) - \frac{2H_3}{L_2 - L_3}(X - 15)}{\lambda_L} + \frac{\frac{2H_3}{L_2 - L_3}(X - 15)}{\lambda_{In}} + \frac{H_2}{\lambda_S} + \frac{1}{h_{S \rightarrow E}}, \quad (2.6b)$$

$$\text{- for } \frac{L_1 - L_3}{2} < X \leq \frac{L_1 + L_3}{2}$$

$$R_{In} = \left(\frac{1}{h_{G \rightarrow L}} + \frac{H_1(i) - H_3}{\lambda_L} + \frac{H_3}{\lambda_{In}} + \frac{H_2}{\lambda_S} + \frac{1}{h_{S \rightarrow E}} \right) \frac{(X - 45)}{(X - 45)}, \quad (2.6c)$$

$$\text{- for } \frac{L_1 + L_3}{2} < X \leq \frac{L_1 + L_2}{2}$$

$$R_{In} = \frac{1}{h_{G \rightarrow L}} + \frac{H_1(i) - H_3 + \frac{2H_3}{L_2 - L_3}(X - 105)}{\lambda_L} + \frac{H_3 - \frac{2H_3}{L_2 - L_3}(X - 105)}{\lambda_{In}} + \frac{H_2}{\lambda_S} + \frac{1}{h_{S \rightarrow E}}, \quad (2.6d)$$

$$\text{- for } \frac{L_1 + L_2}{2} < X \leq L_1$$

$$R_{In} = \left(\frac{1}{h_{G \rightarrow L}} + \frac{H_1(i)}{\lambda_L} + \frac{H_2}{\lambda_S} + \frac{1}{h_{S \rightarrow E}} \right) \frac{(X - 135)}{(X - 135)}. \quad (2.6e)$$

The rate of change η_R in the thermal resistance of the refractory brick based on both with and without the insulation material can be calculated by the following formula.

$$\eta_R = \frac{R_{In}}{R} = 1 + \frac{H_3}{R} \left(\frac{\lambda_L - \lambda_{In}}{\lambda_L \lambda_{In}} \right). \quad (2.7)$$

Regardless of whether the insulation material was included as the lining of the rotary kiln wear, the thermal resistance of the rotary kiln decreased proportionally according to Eqs (2.5)-(2.6). However, after introducing the insulation material, the thermal resistance of the rotary kiln increases greatly compared to the case without the insulation material. In this study, as the lining thickness changed from 230 mm to 80 mm, the rate of change η_R in the thermal resistance increased from 150% to 550%. The extreme importance of the introduction of the insulation material in the rotary kiln is illustrated by the changing trend of the rate despite the wear of the lining.

To evaluate the thermal efficiency of the rotary kiln during wear, in this work, $T_{av}^L(i)/T_{av}^{L+In}(i)$, $T_{av}^S(i)/T_{av}^{S+In}(i)$ and $q_{av}^L(i)/q_{av}^{L+In}(i)$ were used as indicators for analysis. The analysis is carried out based on three cases: (1) independent analysis $\eta_{av}^j(i)$ without insulation material based on refractory brick height $HI(1) = 230\text{mm}$, (2) independent analysis $\eta_{av}^{j+In}(i)$ with insulation material based on refractory brick height $HI(1) = 230\text{mm}$ and (3) comparative analysis $\eta_{av}^{j \leftrightarrow In}(i)$ for both cases with and without the insulation material, where j is L, S and q .

For analysis of case (1), (2) and (3), the following formula can be used to analyze, respectively:

$$\eta_{av}^{L \leftrightarrow In}(i) = \frac{T_{av}^{L+In}(i) - T_{av}^L(i)}{T_{av}^{L+In}(i)}, \quad \eta_{av}^{L+In}(i) = \frac{T_{av}^{L+In}(I) - T_{av}^{L+In}(i)}{T_{av}^{L+In}(I)}, \quad \eta_{av}^L(i) = \frac{T_{av}^L(I) - T_{av}^L(i)}{T_{av}^L(I)}, \quad (2.8)$$

$$\eta_{av}^{S \leftrightarrow In}(i) = \left| \frac{T_{av}^{S+In}(i) - T_{av}^S(i)}{T_{av}^{S+In}(i)} \right|, \quad \eta_{av}^{S+In}(i) = \left| \frac{T_{av}^{S+In}(I) - T_{av}^{S+In}(i)}{T_{av}^{S+In}(I)} \right|, \quad \eta_{av}^S(i) = \left| \frac{T_{av}^S(I) - T_{av}^S(i)}{T_{av}^S(I)} \right|, \quad (2.9)$$

$$\eta_{av}^{q \rightarrow L \leftrightarrow In}(i) = \left| \frac{q_{av}^{L+In}(i) - q_{av}^L(i)}{q_{av}^{L+In}(i)} \right|, \quad \eta_{av}^{q \rightarrow L+In}(i) = \left| \frac{q_{av}^{L+In}(I) - q_{av}^{L+In}(i)}{q_{av}^{L+In}(I)} \right|, \quad (2.10)$$

$$\eta_{av}^{q \rightarrow L}(i) = \left| \frac{q_{av}^L(I) - q_{av}^L(i)}{q_{av}^L(I)} \right|.$$

The VESNA was used to create 3D models, simulate the temperature field of the rotary kiln, and calculate heat flux of the inner surface of the lining with heights of 230 mm, 200 mm, 170 mm, 140 mm, 110 mm and 80 mm for both cases with and without the insulation material. For the calculation, a curvilinear three-dimensional nodal 8-terminal element was used. The grid model for calculating the thermal process in the rotary kiln with the lining height of 230 mm is shown in Fig.2. The total number of finite elements is 216353. Figure 2a shows the grid model of the rotary kiln and Fig.2b shows the lining structure with insulation material.

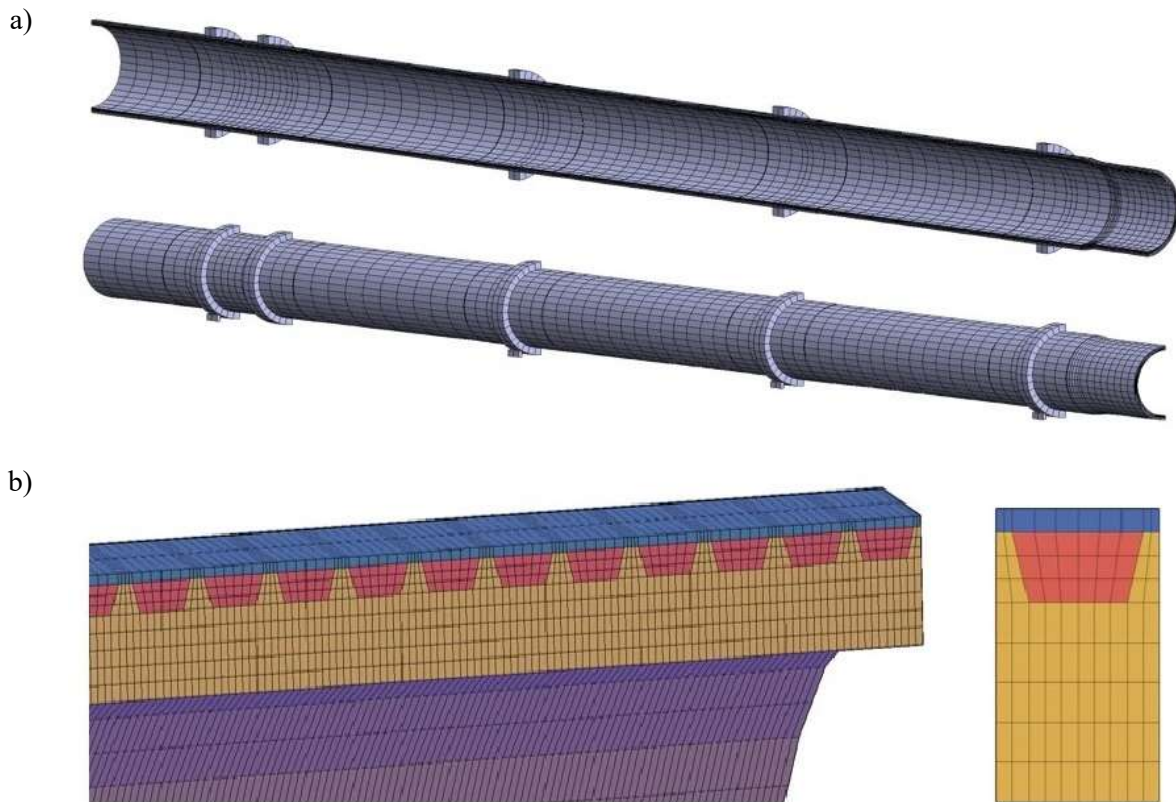


Fig.2. Grid model of the rotary kiln for modeling the thermal process. A total of 216353 finite elements were used.

a) – grid model of the rotary kiln; b) – detailed model of the lining with insulation material.

3. Results and discussion

A simulation is performed [9] on the temperature field based on the wear of the rotary kiln with help of VESNA. Figure 3 shows the results of calculating the temperature fields in the rotary kiln with the lining made of the refractory brick with dimensions of $230 \times 150 \times 74 \text{ mm}$. The insulation material used has dimensions $L2 = 120 \text{ mm}$, $L3 = 90 \text{ mm}$, $H3 = 60 \text{ mm}$ (as shown in Fig.1). For a convenient comparison, the relevant results of both heat flux and temperature are also given based on two cases. As can be seen, the high temperature is distributed on the inner surface of the lining of the rotary kiln, while the low temperature is distributed on the outer surface of the shell of the rotary kiln.

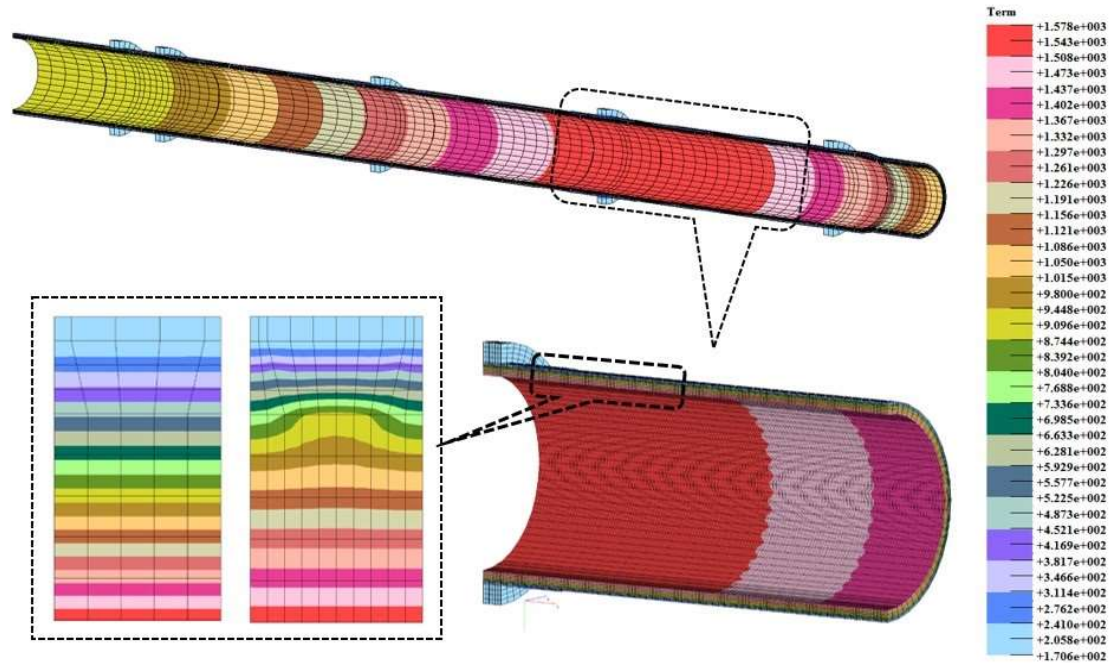


Fig.3. Temperature field of both the rotary kiln and the lining (230 mm) with insulation material and standard refractory bricks (for comparison).

The average temperature and average heat flux of the inner surface of the refractory brick as well as the average temperature of the outer surface of the corresponding shell were chosen as indicators in order to more accurately assess the thermal efficiency of the rotary kiln, while taking the maximum temperature of the lining, shell and insulation material into consideration is quite necessary in a rotary kiln to prevent exceeding the maximum temperature of its own physical properties. The relevant simulation data from VESNA are shown in Tab.2.

As can be seen from Tab.2, as the lining of the rotary kiln gradually becomes thinner due to wear, the average temperature, and maximum temperature of the inner surface of the refractory brick decrease and the average heat flux of the inner surface of the refractory brick, the average temperature and maximum temperature of the outer surface of the corresponding shell increase whether or not it contains the insulation material as shown in Fig.5(a, d, g). Furthermore, the maximum temperature of the insulation material also increases. According to the simulated data of the height $H1$ of the lining of the rotary kiln, here $H1 = 230 \text{ mm}$, 200 mm , 170 mm , 140 mm , 110 mm , and 80 mm , it is shown that the wear of the lining is one of the most important factors affecting its thermal efficiency.

Table 2. The data of the average and maximum temperature and average heat flux.

	Average temperature of the inner surface of the refractory brick		Average temperature of the outer surface of the corresponding shell		Average heat flux of the inner surface of the refractory brick	
	$T_{av}^{L+In}(i)$	$T_{av}^L(i)$	$T_{av}^{S+In}(i)$	$T_{av}^S(i)$	$q_{av}^{L+In}(i)$	$q_{av}^L(i)$
230	1578.76	1534.81	248.27	292.09	4843.25	6599.24
200	1570.1	1516.86	259.28	310.15	5188.74	7316.12
170	1560.04	1494.06	272.04	332.08	5589.06	8227.18
140	1548.36	1464.02	286.28	359.05	6048.63	9427.32
110	1535.61	1422.54	302.74	393.42	6530.81	11084.38
80	1525.95	1361.31	321.67	439.74	6798.93	13530.61

	Maximum temperature of the inner surface of the refractory brick		Maximum temperature of the outer surface of the corresponding shell		Maximum temperature of the insulation material
	$T_{max}^{L+In}(i)$	$T_{max}^L(i)$	$T_{max}^{S+In}(i)$	$T_{max}^S(i)$	$T_{max}^{In}(i) / ^\circ C$
230	1578.83	1534.79	251.1	292.09	961.25
200	1570.33	1516.88	262.36	310.15	1034.01
170	1560.87	1494.08	275.4	332.08	1119.28
140	1551.53	1464.02	289.98	359.05	1220.42
110	1547.74	1422.57	306.85	393.42	1342.87
80	1570.16	1361.33	326.28	439.47	1496.89

With the help of VESNA, the thermal process of the rotary kiln was solved, the temperature field of the rotary kiln was determined, and the maximum temperature of the inner surface of the lining was obtained at $1579^\circ C$ when the height of the lining is 230 mm . This result is in full agreement with that given in the work of Shubin V.I. [28] and is explained by the fact that the technology requires bulk raw materials subjected to a temperature of $1450^\circ C$ for a period of time in the sintering zone. In the sintering zone, the temperature of the hot gas flow is about $1700^\circ C$, and the results are also quite consistent, with an 8% difference from the work of Li *et al.* [29], where the maximum temperature is $1439^\circ C$. The reason for this difference is that this work considered the more extreme case of the rotary kiln. In addition, the lack of processing materials also contributes to the increase in lining temperature.

It is obvious that the thermal resistance of the refractory brick has increased significantly after the introduction of insulation material as shown in Fig.4(a) based on the same conditions. With the help of formula (2.6), it can be calculated that the thermal resistance of the refractory brick with trapezoidal insulation material presents a "hat shape" distribution with length Ll of the refractory brick from 0 mm to 150 mm , as shown in Fig.4(a), while in refractory bricks without trapezoidal insulation material, the thermal resistance of the refractory brick remains unchanged, which can be obtained with the help of formula (2.5) as shown in Fig.4(b).

Thermal resistance refers to the resistance that heat encounters on the heat flow path, reflecting the heat transfer capacity among heat transfer media. The larger the thermal resistance in the refractory brick, the smaller the heat transfer ability. According to the thermal resistance distribution curve of the refractory brick in Fig.4(a, b), it is easy to obtain the condition of the temperature distribution of the inner surface of the refractory brick and the outer surface of the corresponding shell in the length Ll from 0 mm to 150 mm as shown in Fig.4(c, d, e, f).

In refractory bricks containing insulation material, if the thermal resistance of the refractory brick is higher, the temperature of the inner surface of the refractory brick is higher, and the temperature of the outer surface of the corresponding shell is lower. The temperature distribution on the inner surface of the refractory brick is like the thermal resistance distribution of the refractory brick, showing a "hat shape" distribution in the length Ll from 0 mm to 150 mm ; this "hat shape" temperature distribution becomes less and less pronounced, and the temperature on the inner surface of the refractory brick decreases as the wear of the lining,

as shown in Fig.4(c), while the temperature distribution on the outer surface of the corresponding shell is opposite to the thermal resistance distribution of the refractory brick, showing a "pot shape" distribution in the length $L1$ from 0mm to 150mm as shown in Fig.4(e). As the lining wears, this "pot shape" temperature distribution becomes more and more pronounced, and the temperature on the outer surface of the corresponding shell increases. However, in refractory bricks without insulation material, the temperature of the inner surface of the refractory brick and the outer surface of the corresponding shell remains unchanged, respectively, in the length $L1$ from 0mm to 150mm , as shown in Fig.4(d, f).

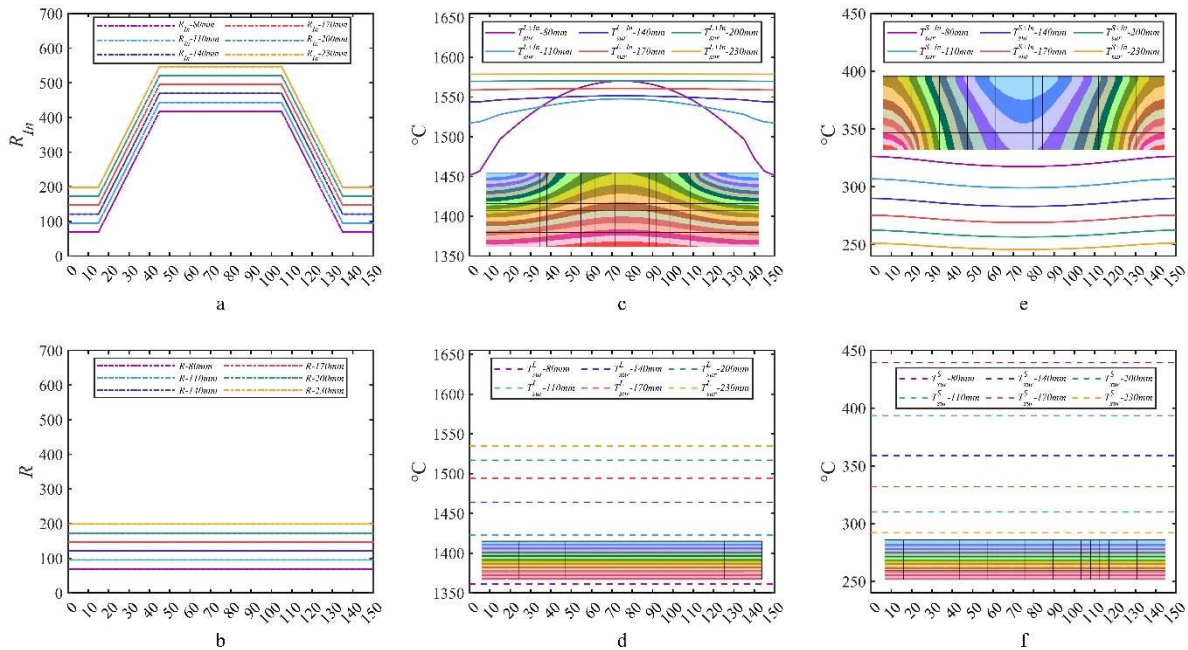


Fig.4. Thermal resistance and temperature of the refractory brick and corresponding shell: a, b - thermal resistance of the refractory brick both with and without the insulation material, c, d - temperature field of the refractory brick both with and without the insulation material, e, f - temperature field of the corresponding shell for the refractory brick both with and without the insulation material.

Table 3. The rate of change in temperature and heat flux.

	The rate of change in the average temperature of the inner surface of the refractory brick			The rate of change in the average temperature of the outer surface of the corresponding shell			The change rate of change in the average heat flux of the inner surface of the refractory brick		
	$\eta_{av}^{L \leftrightarrow In}(i)$	$\eta_{av}^{L+In}(i)$	$\eta_{av}^L(i)$	$\eta_{av}^{S \leftrightarrow In}(i)$	$\eta_{av}^{S+In}(i)$	$\eta_{av}^S(i)$	$\eta_{av}^{q \rightarrow L \leftrightarrow In}(i)$	$\eta_{av}^{q \rightarrow L+In}(i)$	$\eta_{av}^{q \rightarrow L}(i)$
230	2.78	0	0	17.65	0	0	36.26	0	0
200	3.39	0.55	1.17	19.62	4.44	6.19	40.99	7.13	10.86
170	4.23	1.19	2.65	22.07	9.57	13.69	47.20	15.39	24.67
140	5.45	1.93	4.61	25.42	15.31	22.98	55.86	24.89	42.85
110	7.36	2.73	7.31	29.95	21.94	34.69	69.72	34.84	67.96
80	10.79	3.35	11.30	36.62	29.57	50.46	99.01	40.38	105.03

According to Fig.4, the thermal efficiency of the rotary kiln gradually declines when the lining of the rotary kiln wears. Under the same degree of wear of the lining, the thermal efficiency of the rotary kiln after the introduction of the insulation material is higher than that before the introduction of the insulation material.

In this work, the average rate of temperature change on the inner surface of the refractory bricks, the average temperature rate of change on the outer surface of the corresponding shell and the average heat flow rate of change on the inner surface of the refractory bricks were calculated for each of the three cases mentioned above to reasonably analyze and evaluate the thermal efficiency of the rotary kiln during wear of the lining. Table 3 shows the results of the calculation for the three above mentioned cases employing formulas (2.8), (2.9) and (2.10).

The average temperature of the inner surface of the refractory brick decreases as shown in Fig.5(a), while the average heat flux of the inner surface of the refractory brick and the average temperature of the outer surface of the corresponding shell increase as shown in Fig.5(d, g). Compared with the rotary kiln without insulation material, the rotary kiln with insulation material has the following characteristics when the wear degree of the lining is the same (i.e. $H1 = 230\text{ mm}, 200\text{ mm}, 170\text{ mm}, 140\text{ mm}, 110\text{ mm},$ and 80 mm): (1) $T_{av}^L(i) < T_{av}^{L+In}(i)$, $T_{av}^S(i) > T_{av}^{S+In}(i)$ and $q_{av}^L(i) > q_{av}^{L+In}(i)$ as shown in Fig.5(a, d, g), (2) $\eta_{av}^{j+Ln}(i) < \eta_{av}^j(i)$ as shown in Fig.5(b, e, h) and (3) $\eta_{av}^{j \leftrightarrow Ln}(i)$ increases as shown in Fig.5(c, f, i), where j is L, S and q .

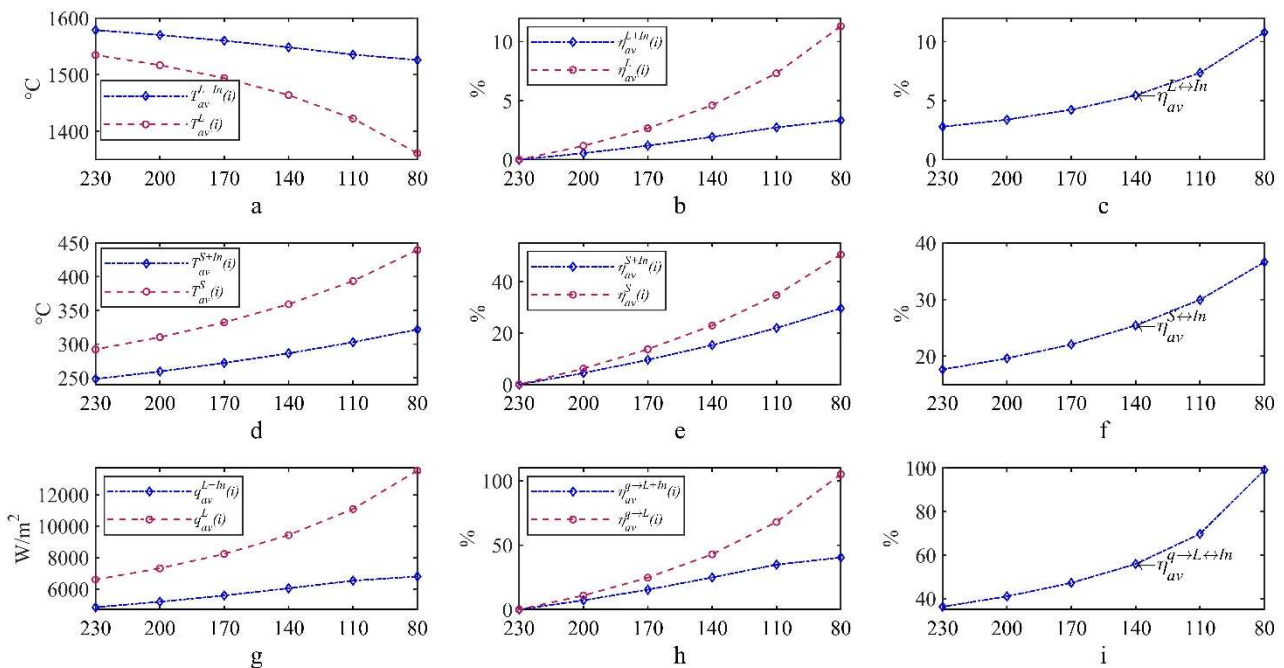


Fig.5. The average temperature and average heat flux and change rate.

It can be observed in Fig.5 that with the wear of the lining, the thermal insulation performance of the lining of the rotary kiln deteriorates and the heat dissipation capacity increases. When the wear of the lining reaches 80 mm in this study, we consider the refractory brick both without and with the insulation material. The average temperature of the inner surface of the refractory brick can be changed by 11.3% and 3.35% , the average heat flux of the inner surface of the refractory brick increases by 105.03% and 40.38% , and the average temperature of the outer surface of the corresponding shell increases by 50.46% and 29.57% . Furthermore, the maximum temperature of the insulation material is 1496.89°C when the lining wear reaches 80 mm , exceeding the maximum physical temperature of 1400°C . The insulation material in the lining has failed due to the maximum temperatures during the operation of the rotary kiln exceeding the maximum temperature of its own physical properties. Thus, the lining of the rotary kiln needs to be regularly inspected and repaired to prevent an increase in energy consumption due to reduced thermal efficiency.

4. Conclusions

In this work, insulation materials with lower thermal conductivity were added into refractory bricks to manufacture more heat-resistant lining. With the help of VESNA, the thermal efficiency of the high-temperature zone of the unloaded 4×60 m rotary kiln was studied, and two cases with and without an insulation material were considered. It can be concluded that: (1) when the refractory bricks do not contain heat insulation material, the maximum temperature in this area is 1534.81°C and the average heat flux on the inner surface of the lining increases by 105.03% when the lining wears to 80 mm; (2) when refractory bricks contain heat insulation materials, the highest temperature in this area is 1578.76°C and the average heat flux on the inner surface of the lining increases by 40.38% when the lining wears to 80 mm; (3) compared to the rotary kiln without the insulation material, the average heat flux on the inner surface of the lining is reduced by 36.26% (230 mm), and the average heat flux on the inner surface of the lining is reduced by 99.01% when the lining is worn to 80 mm. The proposed design solution is conducive to improving the thermal efficiency of the rotary kiln, reducing the overall weight of the rotary kiln, and reducing heat loss to the environment. The obtained results can make contributions to the latest equipment design and improvement of existing equipment.

Prospects for further research.

Further plans include assessing the stress-strain state of the lining and reconfiguring fire-resistant bricks.

Acknowledgements

This work is supported partially by the China Scholarship Council.

Nomenclature

- D_p – the inner diameter of the rotary kiln, m .
- $HI(i)$ – the lining thickness, initial thickness $HI(1)$ is 230 mm.
- $H2$ – the shell thickness, 20 mm.
- $H3$ – the height of the trapezoidal insulation material, 60 mm.
- i – index, $i = 1, 2, \dots, 6$, corresponding to 230 mm, 200 mm, 170 mm, 140 mm, 110 mm and 80 mm.
- $L1$ – the length of the refractory brick, 150 mm.
- $L2$ – the length of the bottom edge of the trapezoidal insulation material, 120 mm.
- $L3$ – the length of the top edge of the trapezoidal insulation material, 60 mm.
- $T_{av}^L(i) / T_{av}^{L+In}(i)$ – the average temperature of the inner surface of the refractory brick based on both without and with insulation material, $^\circ\text{C}$.
- T_G – the temperature of the high-temperature hot gas flow, $^\circ\text{C}$.
- T_{In} – the temperature of the insulation material when in contact with the refractory brick, $^\circ\text{C}$.
- T_L – the temperature of the refractory when in contact with insulation material, $^\circ\text{C}$.
- $T_{L-InnerSur}$ – the temperature of the inner surface of the refractory brick, $^\circ\text{C}$.
- $T_{L-OuterSur}$ – the temperature of the outer surface of the refractory brick, $^\circ\text{C}$.
- $T_{max}^L(i) / T_{max}^{L+In}(i)$ – the maximum temperature of the lining based on both without and with insulation material, $^\circ\text{C}$.
- $T_{max}^{In}(i)$ – the maximum temperature of the insulation material, $^\circ\text{C}$.

- $T_{av}^S(i) / T_{av}^{S+In}(i)$ – average temperature of the outer surface of the corresponding shell based on both without and with insulation material, °C.
- $T_{max}^S(i) / T_{max}^{S+In}(i)$ – the maximum temperature of the corresponding shell based on both without and with insulation material, °C.
- $T_{S-OuterSur}$ – the temperature of the outer surface of the corresponding shell, °C.
- $T_{S-InnerSur}$ – the temperature of the inner surface of the corresponding shell, °C.
- $q_{av}^L(i)$ – the average heat flux of the inner surface of the refractory brick without insulation material.
- $q_{av}^{L+In}(i)$ – the average heat flux of the inner surface of the refractory brick with insulation material.
- W – the circumferential angle of the refractory brick, 2°.
- ω_G – the velocity of the high-temperature hot gas flow.
- ν_G – the viscosity of the high-temperature hot gas flow, m^2 / s ;
- λ_L – the thermal conductivity of the lining, $W/m \cdot K$.
- λ_S – the thermal conductivity of the shell, $W/m \cdot K$.
- λ_{In} – the thermal conductivity of the trapezoidal insulation material, $W/m \cdot K$.
- λ_G – the thermal conductivity of the high-temperature hot gas flow, $W/m \cdot K$.
- ε_L – the emissivity of the refractory brick when $T = TL$.
- ε_G – the emissivity of the high-temperature hot gas flow when $T = TG$.
- $\eta_{av}^{L \leftrightarrow In}(i) / \eta_{av}^{S \leftrightarrow In}(i) / \eta_{av}^{q \leftrightarrow In}(i)$ – are the rate of change of the average temperature of the inner surface of the refractory brick, the average temperature of the outer surface of the corresponding shell and the average heat flux of the inner surface of the refractory brick based on the comparison of the refractory brick with the insulation material with the refractory brick without the insulation material, %.
- $\eta_{av}^{L+In}(i) / \eta_{av}^{S+In}(i) / \eta_{av}^{q+In}(i)$ – the rate of change of the average temperature of the inner surface of the refractory brick, the average temperature of the outer surface of the corresponding shell and the average heat flux of the inner surface of the refractory brick compared with the height of the refractory brick $HI(1) = 230 \text{ mm}$ based on the comparison of the refractory brick with the insulation material, %.
- $\eta_{av}^L(i) / \eta_{av}^S(i) / \eta_{av}^q(i)$ – the rate of change of the average temperature of the inner surface of the refractory brick, the average temperature of the outer surface of the corresponding shell and the average heat flux of the inner surface of the refractory brick compared with the height of the refractory brick $HI(1) = 230 \text{ mm}$ based on compared with the refractory brick without the insulation material, %.

References

- [1] Igliński B. and Buczkowski R. (2017): *Development of cement industry in Poland - History, current state, ecological aspects. A review.* – Journal of Cleaner Production, vol.141, pp.702-720, <https://doi:10.1016/j.jclepro.2016.09.139>.
- [2] Nielsen A.R., Aniol R.W., Larsen M.B., Glarborg P. and Dam-Johansen K. (2011): *Mixing large and small particles in a pilot scale rotary kiln.* – Powder Technology, vol.210, No.3, pp.273-280, <https://doi:10.1016/j.powtec.2011.03.029>.
- [3] Schneider M., Romer M., Tschudin M. and Bolio H. (2011): *Sustainable cement production-present and future.* – Cement and Concrete Research, vol.41, No.7, pp.642-650, <https://doi:10.1016/j.cemconres.2011.03.019>.
- [4] Xu D., Cui Y., Li H., Yang K., Xu W. and Chen Y. (2015): *On the future of Chinese cement industry.* – Cement and Concrete Research, vol.78, pp.2-13, <https://doi:10.1016/j.cemconres.2015.06.012>.
- [5] Gaurav G.K. and Khanam S. (2017): *Computational fluid dynamics analysis of sponge iron rotary kiln.* – Case Studies in Thermal Engineering, vol.9, pp.14-27, <https://doi:10.1016/j.csite.2016.11.001>.

- [6] Piton M., Huchet F., Le Corre O., Le Guen L. and Cazacliu B. (2015): *A coupled thermal-granular model in flights rotary kiln: industrial validation and process design.*– Applied Thermal Engineering, vol.75, pp.1011-1-21, <https://doi.org/10.1016/j.applthermaleng.2014.10.052>.
- [7] Boateng A.A. and Barr P.V. (1996): *A thermal model for the rotary kiln including heat transfer within the bed.*– International Journal of Heat and Mass Transfer, vol.39, pp.2131-2147, [https://doi.org/10.1016/0017-9310\(95\)00272-3](https://doi.org/10.1016/0017-9310(95)00272-3).
- [8] Mittal A. and Rakshit D. (2020): *Energy audit and waste heat recovery from kiln hot shell surface of a cement plant.*– Thermal Science and Engineering Progress, vol.19, pp.100599, <https://doi.org/10.1016/j.tsep.2020.100599>.
- [9] Gürtürk M. and Oztop H.F. (2014): *Energy and exergy analysis of a rotary kiln used for plaster production.*– Applied Thermal Engineering, vol.67, No.1-2, pp.554-565, <https://doi.org/10.1016/j.applthermaleng.2014.03.025>.
- [10] Shcherbina V. and Shvachko D. (2020): *Modeling of the process of non-stationary heat exchange in the lining of a rotating unit.*– CHEERS, vol.2, pp.20-31, <https://doi.org/10.20535/2617-9741.2.2020.208052>.
- [11] Nafsun A.I., Herz F., Specht E., Komossa H., Wirtz S., Scherer V. and Liu X. (2017): *Thermal bed mixing in rotary drums for different operational parameters.*– Chemical Engineering Science, vol.160, pp.346-353, <https://doi.org/10.1016/j.ces.2016.11.005>.
- [12] Nafsun A.I. and Herz F. (2016): *Experiments on the temperature distribution in the solid bed of rotary drums.*– Applied Thermal Engineering, vol.103, pp.1039-1047, <https://doi.org/10.1016/j.applthermaleng.2016.04.128>.
- [13] Villalba Weinberg A., Varona C., Chaucherie X., Goeuriot D. and Poirier J. (2016): *Extending refractory lifetime in rotary kilns for hazardous waste incineration.*– Ceramics International, vol.42, No.15, pp.17626-17634, <https://doi.org/10.1016/j.ceramint.2016.08.078>.
- [14] Slovikovskii V.V. (2008): *Rotary kiln corrosion-erosion-resistant linings.*– Refract Ind. Ceram., vol.49, No.2, pp.99-102, <https://doi.org/10.1007/s11148-008-9034-2>.
- [15] Atmaca A. and Yumrutaş R. (2014): *Analysis of the parameters affecting energy consumption of a rotary kiln in cement industry.*– Applied Thermal Engineering, vol.66, No.1-2, pp.435-444, <https://doi.org/10.1016/j.applthermaleng.2014.02.038>.
- [16] Sharikov Yu.V. and Markus A.A. (2014): *Mathematical modeling of thermal fields in a fragment of the lining of a rotary kiln.*– Metallurgist, vol.57, No.11, pp.1062-1066, <https://doi.org/10.1007/s11015-014-9845-y>.
- [17] Shcherbina V., Shvachko D. and Borshchik S. (2019): *Heat exchange simulation in energy zones of a rotary kiln with change of heat resistance of the body.*– TAPR, vol.60, No.1, pp.36-41, <https://doi.org/10.15587/2312-8372.2019.189169>.
- [18] Trotsenko L. N. (2016): *Features of the design and thermal operation of rotary kilns and promising directions for their improvement.*– Energy Technologies and Resource Saving, vol.4, pp.61-70, URI: <http://dspace.nbu.gov.ua/handle/123456789/159158>
- [19] Yin Q., Du W.J., Ji X.L. and Cheng L. (2017): *Optimization design based on the thermal resistance analyses of heat recovery systems for rotary kilns.*– Applied Thermal Engineering, vol.112, pp.1260-1270, <https://doi.org/10.1016/j.applthermaleng.2016.08.148>.
- [20] Shcherbina V. and Shvachko D. (2022): *The effect of thermal insulation of the lining on the heat exchange of rotating apparatuses.*– CHEERS, vol.2, pp.22-33, <https://doi.org/10.20535/2617-9741.2.2022.260342>.
- [21] Herz F. (2018): *Prozessmodellierung von direkt befeuerten Drehrohröfen zur Beurteilung der thermischen Belastung des Feuerfestmaterials.*– Keramische Zeitschrift, vol.70, No.1, pp.26-35, <https://doi.org/10.1007/s42410-018-0003-1>.
- [22] Li P., Cai L.L., Zhou P.W., Tang D., Zhai P.C. and Zhang Q.J. (2015): *A thermoelectric waste-heat-recovery system for portland cement rotary kilns.*– Journal of Electronic Materials, vol.44, No.6, pp.1750-1762, <https://doi.org/10.1007/s11664-014-3543-1>.
- [23] Alonso E., Gallo A., Roldán M.I., Pérez-Rábago C.A. and Fuentealba E. (2017): *Use of rotary kilns for solar thermal applications: review of developed studies and analysis of their potential.*– Solar Energy, vol.44, pp.90-104, <https://doi.org/10.1016/j.solener.2017.01.004>.
- [24] Byung Soo Joo, Yeon Ha Chang, Hyung Jo Seo and Ho Jang (2019): *Effects of binder resin on tribological properties and particle emission of brake linings.*– Wear, vol.434, vol.435, pp.202195, <https://doi.org/10.1016/j.wear.2019.202995>.

- [25] Roshchupkina I.Yu., Abdrakhimova E.S., Kairakbaev A.K., Abdrakhimov V.Z. and Kolpakov A.V. (2015): *Innovative technology developments aimed at structural-chemical modification of lining materials based on nonferrous metalurgy waste and phosphate binders.*– Refractories and Industrial Ceramics, vol.34, No.4, pp.398-401, <https://doi.org/10.1007/s11148-015-9855-8>.
- [26] Wilson D. Guillin-Estrada, Rafael Albuja, Ivan B. Dávila, Bernardo S. Rueda, Lesme Corredor, Arturo Gonzalez-Quiroga, Heriberto Maury (2022): *Transient operation effects on the thermal and mechanical response of a large-scale rotary kiln.*– Results in Engineering, vol.14, 100396, <https://doi.org/10.1016/j.rineng.2022.100396>.
- [27] Scherbyna V., Gondlyakh A., Sokolskiy A., Shilovich Y. and Bulavina N. (2023): *Failure analysis of refractories in rotary kilns.*– Advanced Manufacturing Processes IV, pp.562-573, https://doi.org/10.1007/978-3-031-16651-8_53.
- [28] Shubin, V.I. (2001): *The effect of temperature on the lining of rotary cement kilns.*– Refractories and Industrial Ceramics, vol.42, pp.216221, <https://doi.org/10.1023/A:1012346718095>.
- [29] Li G., Liu Z., Jiang G., Liu H. and Xiong H. (2015): *Numerical simulation of the influence factors for rotary kiln in temperature field and stress field and the structure optimization.*– Advances in Mechanical Engineering, vol.7, No.6, pp.1-15, <https://doi.org/10.1177/1687814015589667>.

Received: November 14, 2022

Revised: March 7, 2023